J Neuropathol Exp Neurol
Vol. 75, No. 11, November 2016, pp. 1072–1080
doi: 10.1093/jnen/nlw083

ORIGINAL ARTICLE

Effect of Inhibition or Deletion of Neutral Endopeptidase on Neuropathic Endpoints in High Fat Fed/Low Dose Streptozotocin-Treated Mice

Matthew S. Yorek, MS, Alexander Obrosov, BA, Bao Lu, MD, Craig Gerard, MD, Randy H. Kardon, MD, PhD, and Mark A. Yorek, PhD

Abstract

Previously we demonstrated that a vasopeptidase inhibitor of angiotensin converting enzyme and neutral endopeptidase (NEP), a protease that degrades vaso- and neuro-active peptides, improves neural function in diabetic rodent models. The purpose of this study was to determine whether inhibition or deletion of NEP provides protection from neuropathy caused by diabetes with an emphasis on morphology of corneal nerves as a primary endpoint. Diabetes, modeling type 2, was induced in C57Bl/6J and NEP deficient mice through a combination of a high fat diet and streptozotocin. To inhibit NEP activity, diabetic C57Bl/6J mice were treated with candoxatril using a prevention or intervention protocol. Twelve weeks after the induction of diabetes in C57Bl/6J mice, the existence of diabetic neuropathy was determined through multiple endpoints including decrease in corneal nerves in the epithelium and subepithelium layer. Treatment of diabetic C57Bl/6J mice with candoxatril improved diabetic peripheral neuropathy and protected corneal nerve morphology with the prevention protocol being more efficacious than intervention. Unlike C57Bl/6J, mice deficient in NEP were protected from the development of neuropathologic alterations and loss of corneal nerves upon induction of diabetes. These studies suggest that NEP contributes to the development of diabetic neuropathy and may be a treatable target.

Key Words: Candoxatril, Corneal nerves, Diabetes, Diabetic neuropathy, Neutral endopeptidase, Neprilysin.

INTRODUCTION

Peripheral neuropathy is the most common complication of diabetes with no known treatment other than good glycemic control, which only delays the onset and slows progression in type 1 diabetes (1, 2). Failure to identify an effective treatment is in part due to its complex etiology. Diabetic peripheral neuropathy has been described by some investigators to be a disease of the vasculature leading to nerve ischemia and altered nerve function (3–6). Other investigators have proposed that diabetic peripheral neuropathy is caused by a combination of metabolic defects associated with an increased flux of glucose through the aldose reductase pathway leading to a defect in Na^+/K^+-ATPase activity and an alteration of signal transduction pathways in the nerve (7, 8). Additional pathologic contributors to diabetic peripheral neuropathy have been reported to include increased formation of advanced glycation endproducts, reduced neurotrophic support, and increased inflammatory and oxidative stress (9, 10). Overall, these mechanisms are all likely to cause damage to neurons, Schwann cells and the vasculature. Ultimately, relentless damage to the nerve complex and surrounding vasculature leads to diabetic peripheral neuropathy. Given the complex etiology of diabetic peripheral neuropathy, a successful treatment will likely require a combination of early detection, life-style changes and pharmaceutical interventions targeting the mechanisms deemed most responsible for the pathogenesis. Before this can occur, additional studies are needed to determine the most relevant and targetable causes of diabetic peripheral neuropathy.

Neutral endopeptidase (NEP), also known as neprilysin or CD10, degrades a number of vasoactive peptides including natriuretic peptides, adrenomedullin, bradykinin, and calcitonin gene-related peptide (CGRP) (11). NEP is found in many tissues including vascular, liver and renal tissue and its activity is increased by fatty acids and glucose in

From the Department of Veterans Affairs Iowa City Health Care System, Iowa City, IA(MSY, RHK, MAY), Department of Internal Medicine, University of Iowa, Iowa City, IA(AO, MAY), Department of Pediatrics and Medicine, Harvard Medical School, Ina Sue Perlmutter Laboratory, Children's Hospital, Boston, MA(BL), Department of Ophthalmology and Visual Sciences, University of Iowa, Iowa City, IA(RHK), Veterans Affairs Center for the Prevention and Treatment of Visual Loss, Iowa City, IA(RHK, MAY) and Fraternal Order of Eagles Diabetes Research Center, University of Iowa, Iowa City, IA(MAY)

Send correspondence to: Mark A. Yorek, Department of Veterans Affairs Iowa City Health Care System, Room 204, Building 40, Iowa City, IA 52246; E-mail: mark-yorek@uiowa.edu

This work supported in part by the Department of Veterans Affairs, Veterans Health Administration, Office of Research and Development, Rehabilitation Research and Development (Merit Award: RX000889-01 [M.A.Y.] and Iowa City VA Center of Excellence for the Prevention and Treatment of Visual Loss: C9251-C [R.H.K.]) and by National Institute of Diabetes and Digestive and Kidney Diseases Grant DK107339 (M.A.Y.) from NIH.

The content of this article are new and solely the responsibility of the authors and do not necessarily represent the official views of the granting agencies.

The authors have no duality or conflicts of interest to declare.

human microvascular cells (12–16). In the PNS, NEP is located in Schwann cell membranes surrounding dorsal root ganglion cells and nerve fibers (17, 18). In the CNS, NEP is associated with neuronal tissue rather than astrocytes (17). High levels of the enzyme are present in all neonatal and early postnatal Schwann cells. As myelination proceeds, it is gradually suppressed in the majority of cells that form myelin but retained in non-myelin forming cells in the adult animal (18). Kioussi et al (18) found that following axonal damage, NEP is re-expressed distal to the injury. These authors suggest that NEP could play a role in axonal regeneration (18).

Previously, in studies using diabetic rodents we have demonstrated that expression of NEP is increased in vascular tissue and that inhibiting NEP pharmacologically or through deletion improved diabetic neuropathic endpoints, and increased vascular relaxation by epineurial arterioles that provide circulation to the sciatic nerve (19–24). Changes in cornea nerve density have been proposed as an early marker of diabetic peripheral neuropathy (25). In this study using a mouse model of type 2 diabetes, we sought to determine whether inhibiting NEP activity at the onset of hyperglycemia (prevention protocol) or 6 weeks after hyperglycemia (intervention protocol) preserves cornea nerve fiber density and other diabetic neuropathic endpoints. We also examined the effect of diabetes and inhibition/deletion of NEP on the expression of CGRP in corneal nerves. Because CGRP is an important neurotransmitter and potent vasodilator and is associated with nerve regeneration, preserving its expression could improve diabetic neural dysfunction (26–30).

MATERIALS AND METHODS

Materials

Unless stated otherwise all chemicals used in these studies were obtained from Sigma Aldrich Chemical Co. (St. Louis, MO).

Animals

C57Bl/6J wild type mice were purchased from Jackson Laboratories. Breeding pairs of NEP-deficient ($NEP^{-/-}$) mice were provided by Drs. Lu and Gerard and are on the C57Bl/6 background (31). These mice have been bred and a colony created at the Veterans Affairs Medical Center, Iowa City, IO. The C57Bl/6J and $NEP^{-/-}$ mice were age-matched for the studies. Deficiency of NEP activity was confirmed in the $NEP^{-/-}$ mice by measuring the specific activity of NEP in liver homogenates, as described by Ayoub and Melzig (32), with modification (33). Activity of NEP in liver from C57Bl/6 was 0.44 ± 0.01 and was reduced in $NEP^{-/-}$ mice to 0.08 ± 0.01 nM 7-amido-3-methylcoumarin (AMC)/minute/mg protein ($p < 0.001$). Mice were housed in a certified animal care facility and food and water were provided ad libitum. Adequate measures were taken to minimize pain or discomfort and all of the experiments were conducted in accordance with international standards on animal welfare and were compliant with all institutional and National Research Council's guidelines for use of animals (ACURF protocol 1212258).

Male C57Bl/6J and $NEP^{-/-}$ mice at 12 weeks of age were used for these studies. The studies were performed as 2 separate experiments with 10–11 mice in each group. Experiment 1 was done using a group of control and diabetic C57Bl/6J and $NEP^{-/-}$ mice. Experiment 2 was done using control and diabetic C57Bl/6J mice with 2 groups of diabetic mice treated with or without candoxatril (NEP inhibitor). The data were combined for presentation. Two diabetic C57Bl/6J mice were lost during the study. To induce diabetes C57Bl/6J and $NEP^{-/-}$ mice were placed on a high fat diet containing 60% kcal as fat (D12492; Research Diets, New Brunswick, NJ). After 8 weeks on the high fat diet mice were treated with 75 mg/kg streptozotocin (EMD Chemicals, San Diego, CA) followed 3 days later with a second dose of streptozotocin (50 mg/kg). Mice with blood glucose ≥13.8 mM (250 mg/dl) were considered diabetic. Diabetic mice remained on the high fat diet for the 12-week duration of the study. For the candoxatril study 2 of the 3 groups of C57Bl/6J diabetic mice were treated with candoxatril in the diet (300 mg/kg, D15071301 prepared by Research Diets) using a prevention or intervention protocol (Pfizer, New York, NY). The dose of candoxatril used was based on previous studies (19). For the prevention protocol, treatment was started immediately after verification of diabetes. For the intervention protocol treatment was started after 6 weeks of hyperglycemia. The third group of diabetic C57Bl/6J mice served as the untreated diabetic group. The non-diabetic group of C57Bl/6J and $NEP^{-/-}$ mice was maintained on a normal diet for the entire period (Harlan Teklad, no. 7001, Madison, WI).

Glucose Clearance

Prior to behavioral and nerve conduction studies, mice were fasted overnight for study of glucose utilization. Mice were injected i.p. with a saline solution containing 2 g/kg glucose. Immediately prior to the glucose injection and for 120 minutes afterwards blood samples were taken to measure circulating glucose levels (34).

Behavioral Tests

Thermal nociceptive responses in hind paws were measured using the Hargreaves method with instrumentation provided by IITC Life Science (Woodland Hills, CA, model 390G), as previously described in (34).

Motor and Sensory Nerve Conduction Velocity

Mice were anesthetized with Nembutal (75 mg/kg, i.p., Abbott Laboratories, North Chicago, IL) and motor and sensory nerve conduction velocities (m/s) were determined as previously described in (34).

Corneal Innervation

Sub-epithelial corneal nerves were imaged *in vivo* using the Rostock cornea module of the Heidelberg Retina Tomograph (Heidelberg Engineering, Vista, CA) confocal microscope as previously described in (35). Corneal nerve fiber length, defined as the total length of all nerve fibers and

branches (in mm) present in the acquired images standardized for area of the image (in mm^2), was determined for each image by tracing the length of each nerve in the image, summing the total length and dividing by the image area. The corneal fiber length for each mouse was the mean value obtained from the acquired images and expressed as mm/mm^2. Based on receiver operating characteristic curve analysis, corneal nerve fiber length is the optimal morphological parameter of corneal nerves for diagnosing patients with diabetic neuropathy and has the lowest coefficient of variation (36, 37).

After completion of all in vivo analyses, including corneal confocal microscopy, corneas were dissected from the eyes and trimmed around the scleral-limbal region. The cornea was fixed for 30 minutes in Zamboni's fixative, blocked using phosphate-buffered saline (PBS) with 0.2% Triton X-100, 2% goat serum, and 1% bovine serum albumin for 2 hours, and then incubated in the same buffer with anti-neuronal class III β-tubulin mouse monoclonal antibody (Covance, Dedham, MA) and anti-CGRP rabbit polyclonal antibody (Sigma), both at a concentration of 1:1000 overnight at 4 °C. After washing with incubation buffer, the tissue was incubated with Alexa Fluor 488 goat anti-mouse IgG_{2a} and Alexa Fluor 546 goat anti-rabbit IgG (Invitrogen, Eugene, OR) at 1:500 in incubation buffer for 2 hours at room temperature. After washing, the cornea was placed epithelium side up on a microscope slide. Four radial cuts were made and the tissue was carefully covered with a cover slip, mounted with ProLong Gold antifade reagent (Life Technologies, Carlsbad, CA), and sealed with clear nail polish. Images were collected using a Zeiss LSM710 confocal microscope with ZEN Black software and comprised multiple images (Carl Zeiss, Oberkochen, Germany). To image the nerve structure of the entire cornea, neuronal class III β-tubulin was imaged with a 20 × objective (Plan-Apochromat 20 ×/0.8) to make 8 × 8 tile scan z-stacks (3400 × 3400 × 30 μm; 4096 × 4096 × 30 pixel) that were further processed to make maximum projection intensity images. With Imaris version 7.6.4 X64 software (Bitplane, Zurich, Switzerland), the surface option (parameters: smoothing enabled, surface grain size = 0.833 μm per pixel, no background elimination, diameter of the largest sphere = 6.23 μm, thresholding was automatic) was used to determine the total surface area covered by nerves; this is represented as a percentage of the total cornea surface area, as determined by manually tracing the cornea with a closed poly-line, as in previous experiments (28, 29). Further, βIII-tubulin was imaged using a 63× objective (Plan-Apochromat 63 ×/1.4), a 3 × 3 tile scan z-stack (405 × 405 × 30.11 μm; 1536 × 1536 × 78 pixel), with optimum axial resolution to image the epithelial nerves of the cornea. These images were cropped to include only the epithelial nerves and subjected to volume analysis using Imaris version 7.6.4 X64 software (Bitplane) (parameters: smooth was enabled, surface grain size = 0.187 μm, no background elimination was used, diameter of the largest sphere was 0.701 μm, thresholding was automatic). The nerve volume is represented as a percentage of total volume as used for previous experiments (35, 38, 39). To scrutinize the percentage of CGRP in class III β-tubulin labeled nerves of the sub-basal nerves a 40× objective (EC-Plan-Neofluar 40x/1.30 oil) was used to make 3 x 3 tile scan confocal z-stacks (637 × 637 × 30 μm; 1536 × 1536 × 38 pixel). A maximum projection intensity image was used for image analysis (parameters: smooth was enabled; surface grain size = 0.134 μm; no background elimination was used; diameter of the largest sphere = 1.23 μm, thresholding was automatic). Finally, CGRP content in βIII-tubulin was assessed in epithelial nerves using the 63× objective (Plan-Apochromat 63×/1.4) where 2 × 2 tile scan confocal z-stacks (269.77 × 269.77 × 26.66 μm; 2048 × 2048 × 73 pixel). Three-dimensional representations of confocal stacks were reconstructed by volume rendering, where a volume of tissue was defined over the fluorescent staining of both class III β-tubulin and CGRP and used for quantifying percentage of CGRP in corneal epithelial nerves (parameters: smooth was enabled, surface grain size = 0.134 μm, no background elimination was used, diameter of the largest sphere = 1.23 μm, thresholding was manual; βIII-tubulin was 28; CGRP was 112). For presentation purposes, images were adjusted using Imaris and scale bars inserted with Fiji (40).

Skin Intra-Epidermal Nerve Fiber Density

Footpads were fixed in ice-cold Zamboni's fixative for 3 hours, washed in 100 mM PBS overnight, and then in PBS containing increasing amounts of sucrose ie 10%, 15%, and 20%, 3 hours in each solution (41). After washing, the samples were snap frozen in O.C.T. (Sakura Finetek USA, Torrance, CA) and stored at −80 °C. Three longitudinal 30-μm-thick footpad sections were cut using a Reichert-Jung Cryocut 1800 (Leica Microsystems, Nussloch, Germany). Non-specific binding was blocked by 3% goat serum containing 0.5% porcine gelatin and 0.5% Triton X-100 in SuperBlock blocking buffer (Thermo Scientific, Rockford, IL), at room temperature for 2 hours. The sections were then incubated overnight with PGP 9.5 antiserum (UltraClone, Isle of Wight, UK) in 1:400 dilution at 4 °C, after which secondary Alexa Fluor 488 conjugated goat anti-rabbit antibody (Invitrogen) in 1:1000 dilution was applied at room temperature for 1 hour. Sections were then coverslipped with VectaShield mounting medium (Vector Laboratories, Burlingame, CA). Profiles were imaged using a Zeiss LSM710 confocal microscope with a 40× objective and were counted by 2 individual investigators who were masked to the sample identity. All immunoreactive profiles within the epidermis were counted and normalized to epidermal length. Length of the epidermis was determined by drawing a polyline along the contour of the epidermis and recording its length in mm. The number of intra-epidermal nerve fiber profiles was reported per mm length.

Data Analysis

The results are presented as mean ± SE. Comparisons between the groups for body weight, blood glucose, motor and sensory nerve conduction velocities, thermal nociception and intra-epidermal nerve fiber profiles were conducted using a 1-way ANOVA and Bonferroni's pairwise test for multiple comparisons (Prism software; GraphPad, San Diego, CA). A p value of less 0.05 was considered significant.

RESULTS

Data reported in the Table were derived from 2 separate studies, which accounts for the higher number of mice in the C57Bl/6J control and untreated diabetic groups. In the first study there were 4 groups of mice; control and untreated diabetic for C57Bl/6J and NEP$^{-/-}$ mice. The second study consisted of 4 groups of C57Bl/6J mice; control, untreated diabetic and diabetic mice treated with candoxatril using a prevention or intervention protocol, as described in "Materials and Methods" section. Once diabetes was verified, the experimental period was 12 weeks. Experiments were started when the mice were 12 weeks of age. The mean weights of the mice at the beginning of the studies were the same for all groups (Table). At the end of the study period all mice had gained weight. C57Bl/6J untreated diabetic mice and diabetic mice treated with candoxatril in the intervention protocol weighed significantly more than C57Bl/6J control mice. NEP$^{-/-}$ untreated diabetic mice weighed significantly more than NEP$^{-/-}$ control mice. Control and untreated diabetic NEP$^{-/-}$ mice tended to weigh less than control and untreated diabetic C57Bl/6J mice, respectively, but the difference was not statistically significant. Blood glucose levels were increased in C57Bl/6J and NEP$^{-/-}$ diabetic mice compared with their respective control groups and treatment with candoxatril did not influence blood glucose levels.

We have previously reported that inducing diabetes in mice by feeding them a high fat diet followed by streptozotocin caused impaired glucose clearance (38, 39). Data in Figure 1 confirm this finding in diabetic C57Bl/6J and NEP$^{-/-}$ mice and demonstrate that inhibition of NEP with candoxatril or through genetic manipulation did not improve glucose clearance. Glucose clearance was similar for control C57Bl/6J and NEP$^{-/-}$ mice.

Data in the Table show that both motor and sensory nerve conduction velocities, thermal nociception and intra-epidermal nerve fiber density were significantly impacted by diabetes in C57Bl/6J mice. The changes in these endpoints are indicative of diabetic neuropathy. Treating C57Bl/6J diabetic mice with candoxatril significantly improved each of these neuropathic endpoints with the exception of sensory nerve conduction velocity in the candoxatril intervention treatment group. Generally, the candoxatril prevention protocol was more effective than the intervention protocol. Likewise, reducing NEP activity through genetic manipulation prevented the development of diabetic neuropathy in NEP$^{-/-}$ mice as determined by diabetic NEP$^{-/-}$ mice having normal motor and sensory nerve conduction velocity and intra-epidermal nerve fiber density (Table). Thermal nociception in diabetic NEP$^{-/-}$ mice was significantly impaired vs control C57Bl/6J and NEP$^{-/-}$ mice but significantly improved compared with diabetic C57Bl/6J mice (Table).

Decrease in the density of corneal nerves has recently garnered interest as an early marker for diabetic peripheral neuropathy (42–45). In our studies, we focused on whether inhibiting NEP activity with candoxatril or through genetic manipulation would protect corneal nerve morphology in diabetic mice. Using corneal confocal microscopy, a non-invasive approach for imaging corneal nerves in vivo, data in the Table demonstrate that corneal fiber lengths are significantly decreased in diabetic C57Bl/6J mice. Inhibiting NEP activity with candoxatril through prevention and, more importantly, an intervention protocol prevented a significant loss of corneal nerves in diabetic C57Bl/6J mice. Disrupting NEP activity through genetic manipulation also prevented the loss of corneal nerves when NEP$^{-/-}$ were induced with diabetes (Table).

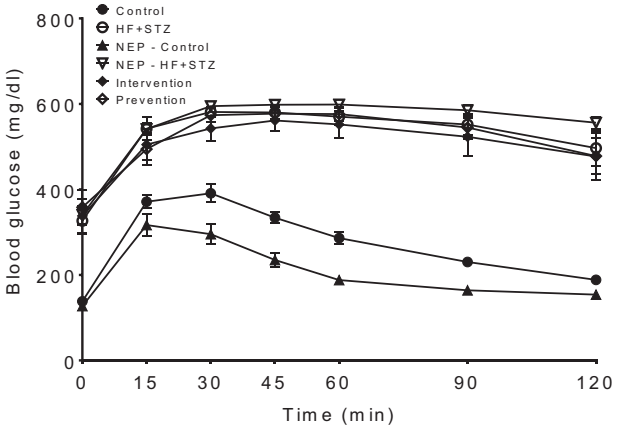

FIGURE 1. Effect on glucose tolerance of high fat/streptozotocin (HF + STZ) induced-diabetes in C57Bl/6J mice with or without treatment of candoxatril (Intervention or Prevention) and NEP$^{-/-}$ mice. Data are presented as mean blood glucose levels in mg/dl ± SE. The area under the curve was significantly different for all diabetic mice vs their respective controls. The number of mice in each group was the same as shown in the Table.

We also investigated the density of corneal nerves in the sub-epithelial and epithelial layers using immunohistochemistry with antibodies to tubulin III and CGRP. Early loss of corneal nerves in the sub-epithelial layer occurs in the region of the whorl in rodents and humans (46–48). Immunostaining for tubulin III or CGRP was decreased in the sub-epithelial layer of diabetic C57Bl/6J mice compared with C57Bl/6J control mice whereas there is no loss of corneal nerves in the sub-epithelial layer of diabetic NEP$^{-/-}$ mice vs control NEP$^{-/-}$ mice (Fig. 2).

Analysis of the entire mouse corneal sub-epithelial layer by immunohistochemical staining for tubulin III revealed that treating diabetic C57Bl/6J mice with candoxatril using a prevention protocol significantly preserved corneal nerves in the sub-epithelial layer in diabetes (Fig. 3). Treating diabetic C57Bl/6J mice with candoxatril using an intervention protocol was less effective than the prevention protocol. The same analyses performed with control and diabetic NEP$^{-/-}$ mice demonstrated that deletion of NEP activity prevented the diabetes-induced decrease in sub-epithelial corneal nerves (Fig. 3).

We previously reported that initial loss of corneal nerves in diabetes occurs in the epithelial layer (49). Figure 4 depicts immunostaining of the distal portion of corneal nerves penetrating the epithelium in the central region of the cornea including the whorl. This figure shows that treating diabetic C57Bl/6J mice with candoxatril protects from distal nerve loss

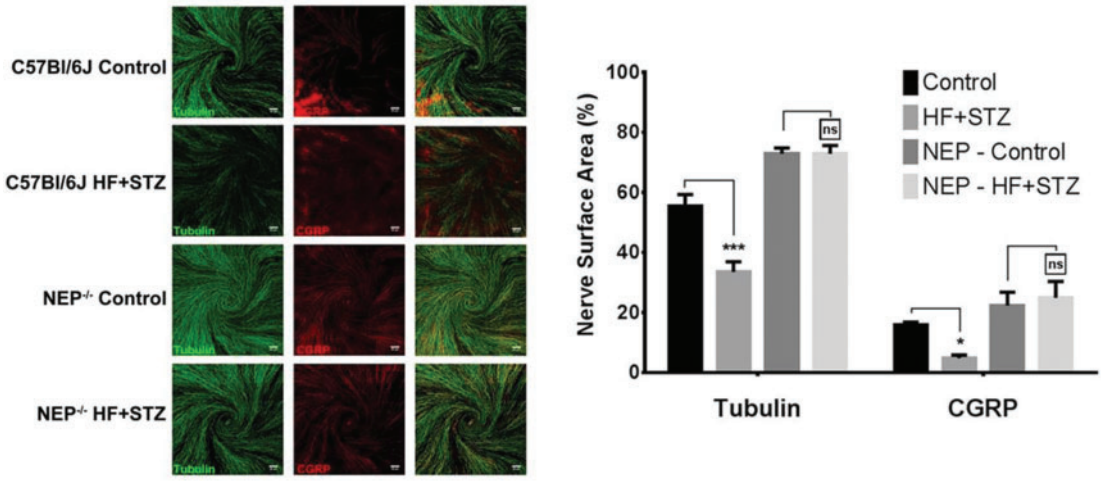

FIGURE 2. The region of the whorl of the sub-epithelial layer of the cornea was examined to determine the effect of high fat/strepto zotocin (HF ± STZ)-induced diabetes in C57Bl/6J or NEP$^{-/-}$ mice on tubulin III and CGRP immunohistochemical staining. Immuno histochemical staining of the corneas *in vitro* was performed as described in "Materials and Methods" section. Representative images are shown for each condition. Imaging was obtained using a 40×/1.3 oil objective (scale bar = 50 μm). Data are presented as the mean ± SE of the surface area covered by nerve staining. Numbers of mice in each group were as shown in the Table. *p < 0.05 vs control; ***p < 0.001 vs control; ns, not significant.

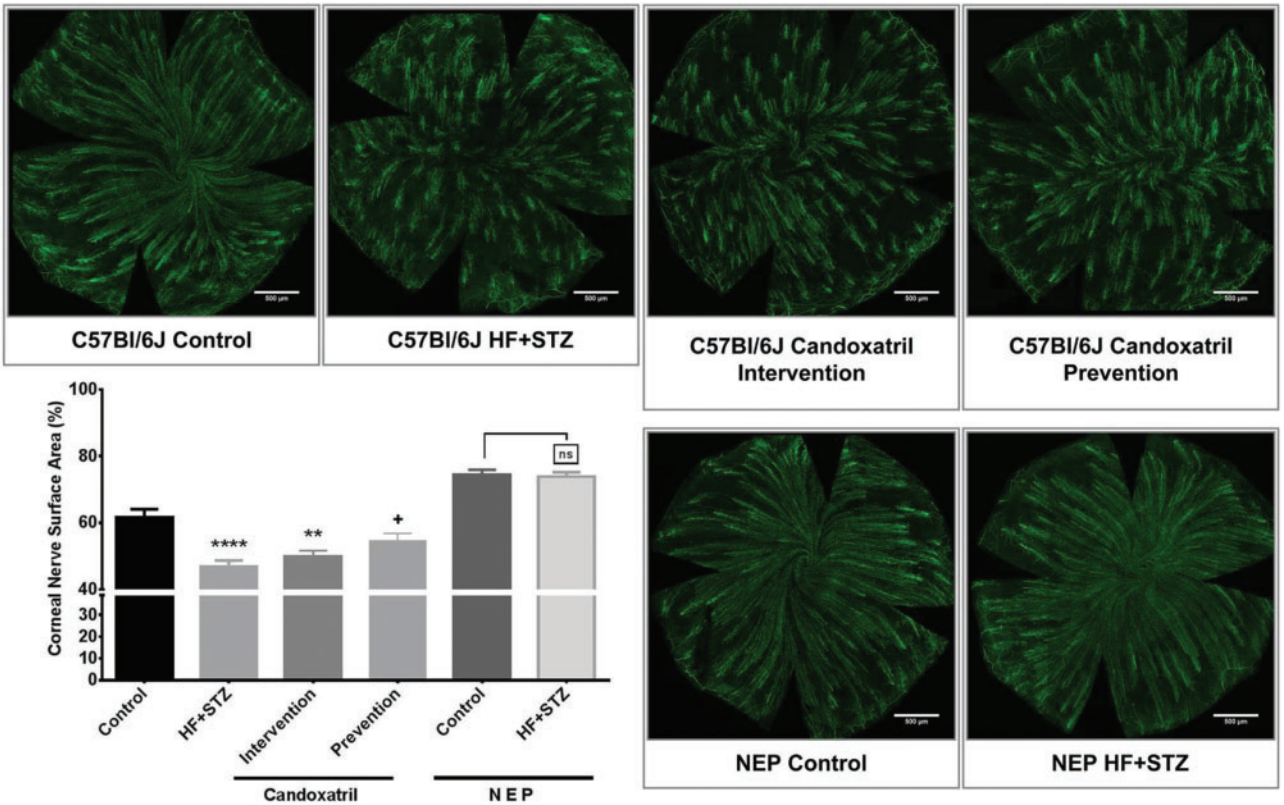

FIGURE 3. The sub-epithelial layers of whole mouse corneas were examined to determine the effect on tubulin III immunohistochemical staining of high fat/streptozotocin (HF + STZ)-induced diabetes in C57Bl/6J with or without treatment of candoxatril and in NEP$^{-/-}$ mice. Representative images are shown for each condition. Imaging was obtained using a 20×/0.8 objective (scale bar = 500 μm). Data are presented as mean ± SE of the surface area covered by nerve staining. Numbers of mice in each group were as shown in the Table. **p < 0.01 vs control; ****p < 0.0001 vs control; +p < 0.05 vs untreated diabetic. Diabetes does not impact the sizes of the corneas (Control and Diabetic, 8.53 ± 0.013 and 8.65 ± 0.12 × 10^6 μm^2, respectively).

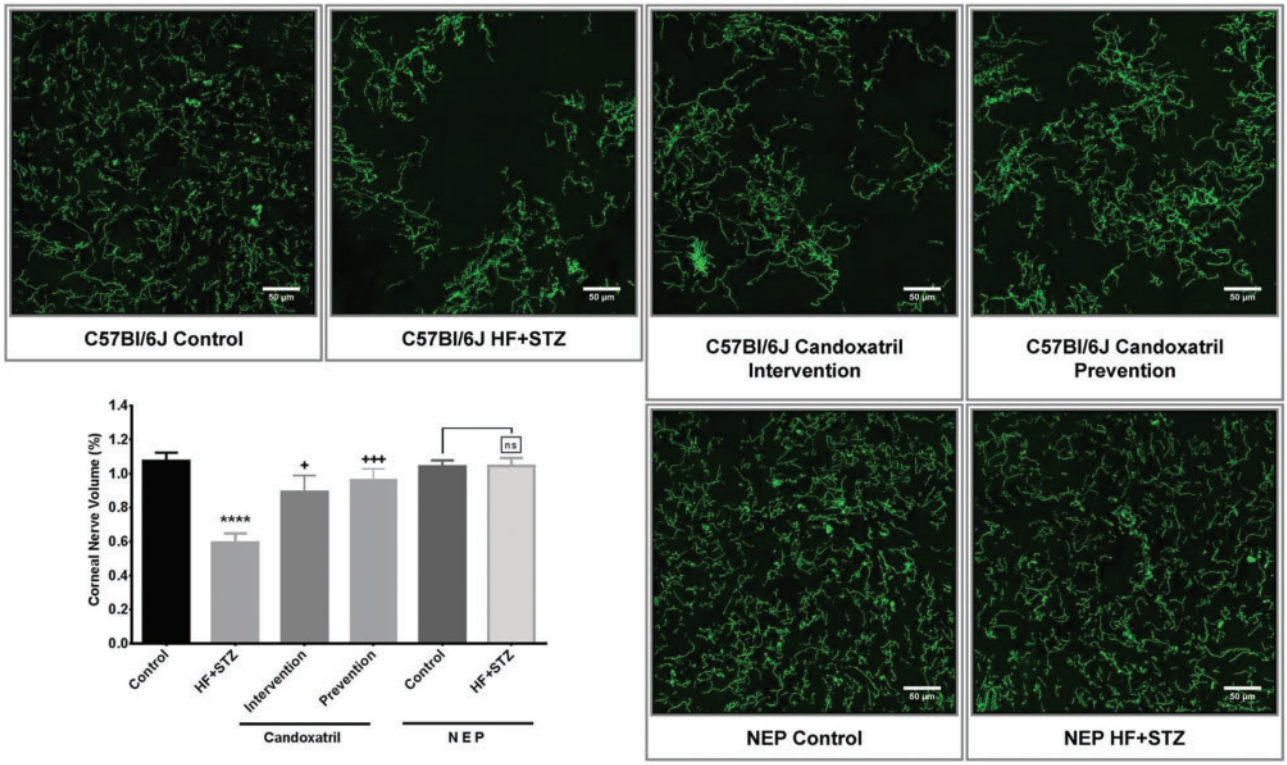

FIGURE 4. The epithelial nerves in the region of the whorl of the cornea were examined to determine the effect on tubulin III immunohistochemical staining of high fat/streptozotocin (HF + STZ)-induced diabetes in C57Bl/6J with or without treatment of candoxatril and NEP$^{-/-}$ mice. Representative images are shown for each condition. Scale bar = 50 μm. Data are presented as the mean ± SE of the volume occupied by nerve staining. The numbers of mice in each group were as shown in the Table. ****$p < 0.0001$ vs control; $^{+}p < 0.05$ vs untreated diabetic; $^{+++}p < 0.001$ vs untreated diabetic.

within the epithelial layer. Diabetic NEP$^{-/-}$ were also protected from nerve loss.

Finally, we examined immunostaining with tubulin III and CGRP of the corresponding corneal nerve bundles of control and diabetic C57Bl/6J mice. Data in Figure 5 demonstrate that diabetes induces a significant loss of tubulin III nerves and that they are protected by inhibiting NEP activity with candoxatril. Furthermore, the loss of CGRP-containing nerves follows a similar trend as tubulin III; however, the loss was not significant.

DISCUSSION

The purpose of these studies was to determine the individual role of NEP on nerve complications that occur in high fat fed/low dose streptozotocin-diabetic mice, a model of late stage type 2 diabetes (38, 39). Because loss of corneal nerves has recently been promoted to be a possible marker of development of diabetic peripheral neuropathy we focused on changes in the morphology of these nerves in the cornea epithelium and sub-epithelial layer as a primary endpoint (25, 42–45). We had previously demonstrated that inhibition of NEP activity in diabetic rodents improved neuropathy, as determined by evaluation of nerve conduction velocity (20, 23, 50). However, little is known whether inhibition of NEP can protect corneal nerves from diabetes. In addition to the potential role of NEP inhibition singularly or in combination with angiotensin activity blockade as a treatment of diabetic neuropathy, other investigations have implicated inhibition of NEP as a treatment for heart failure, hypertension, chronic renal disease and wound healing (51–56). Thus, increasing our understanding of the impact of NEP activity in chronic diseases may lead to improved treatments.

The major findings of this study were that pharmacological inhibition of NEP or silencing NEP activity by genetic manipulation reduced the impact of 12 weeks of diabetes on endpoints associated with neuropathy including motor and to a lesser extent sensory nerve conduction velocity, intra-epidermal nerve fiber density and density of corneal nerves in the epithelium and sub-epithelial layer. The lone exception was that in this study using a mouse model of type 2 diabetes we found that hypoalgesia was significantly improved in diabetic NEP$^{-/-}$ mice compared with diabetic C57Bl/6J mice; thermal nociception remained significantly impaired compared with control C57Bl/6J and NEP$^{-/-}$ mice. This result differs from our previous studies using type 1 diabetic or diet-induced obesity C57Bl/6J and NEP$^{-/-}$ mice (19, 33, 34). This occurred even though the intra-epidermal nerve fiber density was not decreased by diabetes in NEP$^{-/-}$ mice. The reason for this is not entirely clear but could be due to signaling pathways responsible for thermal sensitivity that are impaired to a greater extent by type 2 diabetes than type 1 diabetes and are

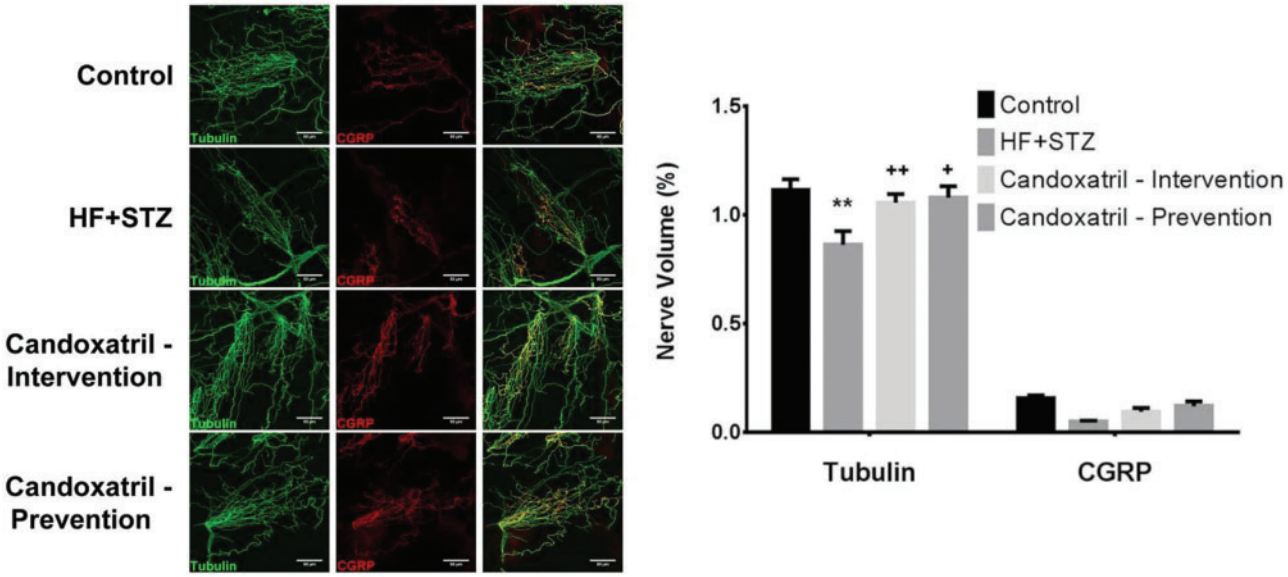

FIGURE 5. Cornea peripheral nerve bundles were examined to determine the effect on tubulin III and CGRP immunohistochemical staining of high fat/streptozotocin (HF + STZ)-induced diabetes in C57Bl/6J with or without treatment of candoxatril. Representative images are shown for each condition. Scale bar = 50 μm. Data are presented as the mean ± SE of the volume occupied by nerve staining. The numbers of mice in each group were as shown in the Table. **$p < 0.01$ vs control; $^{+}p < 0.05$ vs untreated diabetic; $^{++}p < 0.01$ vs untreated diabetic.

independent of NEP activity. Inhibition of NEP activity by candoxatril in diabetic C57Bl/6J mice also did not completely prevent latency in thermal sensitivity or the decrease in nerve conduction velocity. Not surprisingly, treating diabetic C57Bl/6J mice with candoxatril using the prevention protocol was generally more effective in protecting diabetic mice from neuropathy than the intervention protocol. However, the 6-week intervention protocol was effective in slowing progression or reversing some diabetic neuropathic endpoints when treatment was initiated after 6 weeks of untreated diabetes. The beneficial effects of inhibiting NEP activity or genetic modification of NEP activity on diabetic neuropathy occurred even though blood glucose levels and glucose utilization were not improved.

We employed multiple approaches to examine the impact of diabetes and inhibition of NEP activity on corneal nerve fiber loss. Corneal confocal microscopy is a non-invasive procedure to examine corneal fiber morphology in the sub-epithelial layer that is being used in both human and animal research. However, *in vivo* corneal confocal microscopy is unable to image corneal nerves that penetrate the epithelium and probably only visualizes a subset of sub-epithelial nerves. The distal portion of corneal nerves within the epithelium is most likely affected the earliest in diabetic neuropathy. At this time, corneal nerves within the epithelium can only be visualized *in vitro* using immunohistochemical staining of the fibers. In this study, we used immunohistochemistry for tubulin III and CGRP to examine corneal nerves. In the corneal nerves of the mouse, CGRP and substance P are the most abundant neuropeptides and both are degraded by NEP (57–61). *In vitro* analysis of tubulin III immunoreactivity in corneal nerves from control and diabetic C57Bl/6J and $NEP^{-/-}$ mice generally supported the results obtained with corneal confocal microscopy. Comparing density of corneal nerves in non-diabetic C57Bl/6J and $NEP^{-/-}$ mice there was a trend for $NEP^{-/-}$ mice to have an increased corneal nerve density whether analyzed by corneal confocal microscopy or immunohistochemically although the difference was not statistically significant. We attribute this to the increase in levels of calcitonin gene-related peptide that is apparent in corneal nerves from $NEP^{-/-}$ mice vs C57Bl/6J mice. As discussed below calcitonin gene-related peptide could promote an increase nerve generation/elongation.

Diabetes in C57Bl/6J mice reduced tubulin III immunoreactivity in both the epithelium and sub-epithelial layer, which was partially protected by treating diabetic mice with candoxatril. Immunoreactivity of tubulin III in both the epithelium and sub-epithelial layer was not reduced by diabetes in $NEP^{-/-}$ mice. A similar result was obtained for immunoreactivity for calcitonin gene-related peptide in control and diabetic C57Bl/6J and $NEP^{-/-}$ mice. Immunoreactivity for calcitonin gene-related peptide was decreased in the sub-epithelial layer of diabetic C57Bl/6J mice but not in diabetic $NEP^{-/-}$ mice. Calcitonin gene-related peptide is a major neurotransmitter found in nerves within the CNS and PNS (62). It is primarily synthesized in the cell bodies of dorsal root and trigeminal ganglion and transported axonally to the nerve fibers and has been recognized as a nerve regeneration-promoting peptide (30, 63–66). It has been shown that expression of the neuropeptides calcitonin gene-related peptide and substance P increase in the early stages of sciatic or sural nerve injury (27, 67, 68). Together, these data suggest that preservation of calcitonin gene-related peptide levels could be beneficial for maintaining nerve integrity and regeneration properties. Thus, one possible role for

TABLE. Effects of Type 2 Diabetes in C57Bl/6J and Neutral Endopeptidase-Deficient Mice

Determination	C57Bl/6J Control (20)	C57Bl/6J Diabetic (18)	C57Bl/6J Diabetic + Candoxatril Intervention (11)	C57Bl/6J Diabetic + Candoxatril Prevention (11)	NEP$^{-/-}$ Control (10)	NEP$^{-/-}$ Diabetic (11)
Start weight (g)	25.6 ± 0.3	26.4 ± 0.4	26.0 ± 0.5	25.2 ± 0.4	26.6 ± 0.4	26.6 ± 0.5
Final weight (g)	33.0 ± 0.5	40.7 ± 2.0[a,c]	42.9 ± 3.6[a,c]	39.8 ± 3.6[c]	28.7 ± 0.7[b]	36.4 ± 2.0[c]
Blood glucose (mg/dl)	186 ± 3	352 ± 26[a]	345 ± 40[a]	347 ± 32[a]	235 ± 8[b]	400 ± 28[a,c]
Motor nerve conduction velocity (m/s)	42.4 ± 1.3	25.5 ± 1.2[a]	37.8 ± 1.5[b]	37.4 ± 1.2[b]	38.2 ± 1.3[b]	38.7 ± 1.7[b]
Sensory nerve conduction velocity (m/s)	27.8 ± 0.7	22.6 ± 0.4[a]	24.5 ± 0.4[a,c,d]	25.1 ± 0.6[b,c,d]	28.4 ± 0.6[b]	29.1 ± 0.8[b]
Thermal nociception (s)	5.2 ± 0.1	8.8 ± 0.1[a]	6.3 ± 0.1[a,b,c]	6.0 ± 0.1[a,b,c]	4.5 ± 0.1[a,b]	6.9 ± 0.2[a,b,c]
Intraepidermal nerve fiber density (profiles/mm)	25.2 ± 0.5	15.6 ± 0.5[a]	20.5 ± 0.5[a,b,c]	22.2 ± 0.7[a,b]	23.9 ± 0.8[b]	22.5 ± 0.5[a,b]
Corneal Confocal Microscopy (mm/mm^2)	2.8 ± 0.2	1.0 ± 0.2[a]	2.2 ± 0.2[b]	2.6 ± 0.3[b]	3.5 ± 0.3[b]	3.6 ± 0.3[b]

Data are presented as the mean ± SE.
[a] $p < 0.05$ compared with C57Bl/6J control.
[b] $p < 0.05$ compared with C57Bl/6J Diabetic.
[c] $p < 0.05$ compared with NEP Control.
[d] $p < 0.05$ compared with NEP Diabetic. Parentheses indicate the number of experimental animals. NEP, neutral endopeptidase.

inhibitors of NEP in the protection of nerve morphology and activity in diabetes is through preventing the degradation of calcitonin gene-related peptide.

In summary, we have demonstrated that attenuating the activity of NEP serves as a potential treatment of diabetic neuropathy perhaps through preservation of important neuropeptides such as CGRP and substance P.

ACKNOWLEDGEMENT

The authors would like to extend their appreciation to Pfizer for supplying candoxatril, for this study.

REFERENCES

1. Kim H, Kim JJ, Yoon YS. Emerging therapy for diabetic neuropathy: cell therapy targeting vessels and nerves. Endocr Metab Immune Disord Drug Targets 2012;12:168–78
2. Figueroa-Romero C, Sadidi M, Feldman EL. Mechanisms of disease: the oxidative stress theory of diabetic neuropathy. Rev Endocr Metab Disord 2008;9:301–14
3. Cameron NE, Cotter MA, Low PA. Nerve blood flow in early experimental diabetes in rats: relation to conduction deficits. Am J Physiol 1991;261:E1–8
4. Nukada H, Dyck PJ. Microsphere embolization of nerve capillaries and fiber degeneration. Am J Pathol 1984;115:275–87
5. Cameron NE, Cotter MA, Dines KC, et al. Aldose reductase inhibition, nerve perfusion, oxygenation and function in streptozotocin-diabetic rats: dose-response considerations and independence from a myo-inositol mechanism. Diabetologia 1994;37:651–63
6. Cameron NE, Cotter MA, Archibald V, et al. Anti-oxidant and pro-oxidant effects on nerve conduction velocity, endoneurial blood flow and oxygen tension in non-diabetic and streptozotocin-diabetic rats. Diabetologia 1994;37:449–59
7. Cotter MA, Dines KC, Cameron NE. Prevention and reversal of motor and sensory peripheral nerve conduction abnormalities in streptozotocin-diabetic rats by the prostacyclin analogue iloprost. Naunyn Schmiedebergs Archives Pharm 1993;347:534–40
8. Cameron NE, Cotter MA, Dines KC, et al. Effects of aminoguanidine on peripheral nerve function and polyol pathway metabolites in streptozotocin-diabetic rats. Diabetologia 1992;35:946–50
9. Sima AA. Pathological mechanisms involved in diabetic neuropathy: can we slow the process? Curr Opin Invest Drugs 2006;7:324–37
10. Pop-Busui R, Sima A, Stevens M. Diabetic neuropathy and oxidative stress. Diabetes Metab Res Rev 2006;22:257–73
11. Pu Q, Schiffrin EL. Effect of ACE/NEP inhibition on cardiac and vascular collagen in stroke-prone spontaneously hypertensive rats. Am J Hypertens 2001;14:1067–72
12. Ebihara F, Di Marco GS, Juliano MA, et al. Neutral endopeptidase expression in mesangial cells. J Renin-Angiotensin-Aldosterone Syst 2003;4:228–33
13. Vatter H, Schilling L, Schmiedek P, et al. Evidence for functional endothelin-converting enzyme activity in isolated rat basilar artery: effect of inhibitors. J Cardiovasc Pharmaco 1998;31:S64–7
14. Muangman P, Spenny ML, Tamura RN, et al. Fatty acids and glucose increase neutral endopeptidase activity in human microvascular endothelial cells. Shock 2003;19:508–12
15. Edwards RM, Pullen M, Nambi P. Distribution of neutral endopeptidase activity along the rat and rabbit nephron. Pharmacology 1999;59:45–50
16. Gonzalez W, Soleilhac JM, Fournie-Zaluski MC, et al. Characterization of neutral endopeptidase in vascular cells, modulation of vasoactive peptide levels. Eur J Pharmacol 1998;345:323–31
17. Matsas R, Kenny AJ, Turner AJ. An immunohistochemical study of endopeptidase-24.11 ("enkephalinase") in the pig nervous system. Neuroscience 1986;18:991–1012
18. Kioussi C, Mamalaki A, Jessen K, et al. Expression of endopeptidase-24.11 (common acute lymphoblastic leukaemia antigen CD10) in the sciatic nerve of the adult rat after lesion and during regeneration. Eur J Neurosci 1995;7:951–61
19. Coppey L Lu B, Gerard C, et al. Effect of inhibition of angiotensin-converting enzyme and/or neutral endopeptidase on neuropathy in high-fat-fed C57Bl/6J mice. J Obes 2012;2012:326806
20. Oltman CL, Davidson EP, Coppey LJ, et al. Role of the effect of inhibition of neutral endopeptidase on vascular and neural complications in streptozotocin-induced diabetic rats. Eur J Pharmacol 2011;15:556–62
21. Oltman CL, Davidson EP, Coppey LJ, et al. Treatment of Zucker fatty rats with AVE7688 improves vascular and neural dysfunction. Diabetes Obes Metab 2009;11:223–33
22. Davidson EP, Kleinschmidt TL, Oltman CL, et al. Treatment of streptozotocin-induced diabetic rats with AVE7688, a vasopeptidase inhibitor: effect on vascular and neural disease. Diabetes 2007;56:355–62
23. Davidson EP, Coppey LJ, Holmes A, et al. Effect of inhibition of angiotensin converting enzyme and/or neutral endopeptidase on vascular and neural complications in high fat fed/low dose streptozotocin-diabetic rats. Eur J Pharmacol 2012;677:180–7
24. Davidson EP, Coppey LJ, Holmes A. Effect of treatment of high fat fed/low dose streptozotocin-diabetic rats with Ilepatril on vascular and neural complications.2011. Eur J Pharmcol 2011;668:497–506

25. Quattrini C, Tavakoli M, Jeziorska M, et al. Surrogate markers of small fiber damage in human diabetic neuropathy. Diabetes 2007;56:2148–54
26. Rosa E, Cha J, Bain JR, et al. Calcitonin gene-related peptide regulation of glial cell-line derived neurotrophic factor in differentiated rat myotubes. J Neurosci Res 2015;93:514–20
27. Fu C, Yin Z, Yu D, et al. Substance P and calcitonin gene-related peptide expression in dorsal root ganglia in sciatic nerve injury rats. Neural Regen Res 2013;8:3124–30
28. Hashhikawa-Hobara N, Hashikawa N, Zamami Y, et al. The mechanism of calcitonin gene-related peptide-containing nerve innervation. J Pharmacol Sci 2012;119:117–21
29. Cortina MS, He J, Li N, et al. Recovery of corneal sensitivity, calcitonin gene-related peptide-positive nerves, and increased wound healing induced by pigment epithelial-derived factor plus docosahexaenoic acid after experimental surgery. Arch Ophthalmol 2012;130:76–83
30. Toth CC, Willis D, Twiss JL, et al. Locally synthesized calcitonin gene-related peptide has a critical role in peripheral nerve regeneration. J Neuropathol Exp Neurol 2009;68:326–37
31. Lu B, Gerard NP, Kolakowski LF. Jr., et al. Neutral endopeptidase modulation of septic shock. J Exp Med 1995;181:2271–5
32. Ayoub S, Melzig MF. Induction of neutral endopeptidase (NEP) activity of SK-N-SH cells by natural compounds from green tea. J Pharm Pharmacol 2005;58:495–501
33. Davidson E, Coppey L, Lu B, et al. The roles of streptozotocin neurotoxicity and neutral endopeptidase in murine experimental diabetic neuropathy. Exp Diabetes Res 2009;2009:431980
34. Coppey L, Davidson E, Lu B, et al. Vasopeptidase inhibitor ilepatril (AVE7688) prevents obesity- and diabetes-induced neuropathy in C57Bl/6J mice. Neuropharmacology 2011;60:259–66
35. Yorek MS, Obrosov A, Shevalye H, et al. Effect of glycemic control on corneal nerves and peripheral neuropathy in streptozotocin-induced diabetic C57Bl/6J mice. J Peripher Nerv Syst 2014;19:205–17
36. Malik RA, Kallinikos P, Abbott CA, et al. Corneal confocal microscopy: a non-invasive surrogate of nerve fibre damage and repair in diabetic patients. Diabetologia 2003;46:683–8
37. Tavakoli M, Kallinikos P, Iqbal A, et al. Corneal confocal microscopy detects improvement in corneal nerve morphology with an improvement in risk factors for diabetic neuropathy. Diabet Med 2011;28:1261–7
38. Yorek MS, Obrosov A, Shevalye H, et al. Effect of diet-induced obesity or type 1 or type 2 diabetes on corneal nerves and peripheral neuropathy in C57Bl/6J mice. J Peripher Nerv Syst 2015;20:24–31
39. Shevalye H, Yorek MS, Coppey LJ, et al. Effect of enriching the diet with menhaden oil or daily treatment with resolvin D1 on neuropathy in a mouse model of type 2 diabetes. J Neurophysiol 2015;114:199–208
40. Schindelin J, Arganda-Carreras I, Frise E, et al. Fiji: an open-source platform for biological-image analysis. Nat Methods 2012;9:676–82
41. Stavniichuk R, Shevalye H, Lupachyk S, et al. Peroxynitrite and protein nitration in the pathogenesis of diabetic peripheral neuropathy. Diabetes Metab Res Rev 2014;30:669–78
42. Azmi S, Ferdousi M, Petropoulos IN, et al. Corneal confocal microscopy identifies small-fiber neuropathy in subjects with impaired glucose tolerance who develop type 2 diabetes. Diabetes Care 2015;38:1502–8
43. Asghar O, Petropoulos IN, Alam U, et al. Corneal confocal microscopy detects neuropathy in subjects with impaired glucose tolerance. Diabetes Care 2014;37:2643–6
44. Tavakoli M, Petropoulos IN, Malik RA. Assessing corneal nerve structure and function in diabetic neuropathy. Clin Exp Optom 2012;95:338–47
45. Edwards K, Pritchard N, Vagenas D, et al. Utility of corneal confocal microscopy for assessing mild diabetic neuropathy: baseline findings of the LANDMark study. Clin Exp Optom 2012;54
46. Davidson EP, Coppey LJ, Kardon RH, et al. Differences and similarities in development of corneal nerve damage and peripheral neuropathy in diet-induced obesity and type 2 diabetic rats. Invest Ophthalmol Vis Sci 2014;55:1222–30
47. Pritchard N, Dehghani C, Edwards K, et al. Utility of assessing nerve morphology in central cornea versus whorl area for diagnosing diabetic peripheral neuropathy. Cornea 2015;34:756–61
48. Petropoulos IN, Ferdousi M, Marshall A, et al. The inferior whorl for detecting diabetic peripheral neuropathy using corneal confocal microscopy. Invest Ophthalmol Vis Sci 2015;56:2498–504
49. Davidson EP, Coppey LJ, Yorek MA. Early loss of innervation of cornea epithelium in streptozotocin-induced type 1 diabetic ras: improvement with ilepatril treatment. Invest Ophthalmol Vis Sci 2012;53:8067–74
50. Yorek MA. The potential role of angiotensin converting enzyme and vasopeptidase inhibitors in the treatment of diabetic neuropathy. Curr Drug Targets 2008;9:77–84
51. Prenner SB, Shah SJ, Yancy CW. Role of angiotensin receptor-neprilysin inhibition in heart failure. Curr Atheroscler Rep 2016;18:48
52. Bavishi C, Messerli FH, Kadosh B, et al. Role of neprilysin inhibitor combinations in hypertension: insights from hypertension and heart failure trials. Eur Heart J 2015;36:1967–73
53. von Lueder TG, Atar D, Krum H. Current role of neprilysin inhibitors in hypertension and heart failure. Pharmacol Ther 2014;144:41–9
54. Judge P, Haynes R, Landray MJ, et al. Neprilysin inhibition in chronic kidney disease. Nephrol Dial Transplant 2015;30:738–43
55. Spenny ML, Muangman P, Sullivan SR, et al. Neutral endopeptidase inhibition in diabetic wound repair. Wound Repair Regen 2002;10:295–301
56. Olerud JE, Usui ML, Seckin D, et al. Neutral endopeptidase expression and distribution in human skin and wounds. J Invest Dermatol 1999;112:873–81
57. Jiucheng H, Bazan HEP. Neuroanatomy and neurochemistry of mouse cornea. Cornea 2016;57:664–74
58. Schlereth T, Breimhorst M, Werner N. Inhibition of neuropeptide degradation suppresses sweating but increases the area of the axon reflex flare. Exp Dermatol 2013;22:299–301
59. Kramer HH, He L, Lu B, et al. Increased pain and neurogenic inflammation in mice deficient of neutral endopeptidase. Neurobiol Dis 2009;35:177–83
60. Kramer HH, Schmidt K, Leis S, et al. Angiotensin converting enzyme has an inhibitory role in CGRP metabolism in human skin. Peptides 2006;27:917–20
61. Leal EC, Carvalho E, Tellechea A, et al. Substance P promotes would healing in diabetes modulating inflammation and macrophage phenotype. Am J Pathol 2015;185:1638–48
62. Yang Q, Du X, Fang Z, et al. Effect of calcitonin gene-related peptide on the neurogenesis of rat adipose-derived stem cells in vitro. Plos One 2014;9:e86334
63. Kashihara Y, Sakaguchi M, Kuno M. Axonal transport and distribution of endogenous calcitonin gene-related peptide in rat peripheral nerve. J Neurosci 1989;9:3796–802
64. Karsan N, Goadsby PJ. CGRP mechanism antagonists and migraine management. Curr Neurol Neurosci Rep 2015;15:25
65. Blesch A, Tuszynski MH. GDNF gene delivery to injured adult CNS motor neurons promotes axonal growth, expression of the trophic neuropeptide CGRP, and cellular protection. J Comp Neurol 2001;436:399–410
66. Chen LJ, Zhang FG, Li J, et al. Expression of calcitonin gene-related peptide in anterior and posterior horns of the spinal cord after brachial plexus injury. J Clin Neurosci 2010;17:87–91
67. Zhang L, Lv X, Tong X, et al. Study on molecular mechanism for improving neural regeneration after repair of sciatic nerve defect in rat by acellular nerve allograft. Synapse 2012;66:52–60
68. Li XQ, Verge VM, Johnston JM, et al. CGRP peptide and regenerating sensory axons. J Neuropathol Exp Neurol 2004;63:1092–103